Biochimica et Biophysica Acta 862 (1986) 27–38
Elsevier

BBA 73315

Potential dependence of unidirectional chloride fluxes across isolated frog skin

Thomas U.L. Biber, John A. DeSimone and Krystyna Drewnowska

Department of Physiology & Biophysics, Medical College of Virginia, Richmond, VA 23298 (U.S.A.)

(Received 28 July 1986)

Key words: Chloride flux; Electrodiffusion; Surface potential; Active transport; Na^+ dependence; (Frog skin)

Isolated frog skins were voltage clamped at transepithelial potentials (V_t) ranging from −60 mV to 60 mV to measure transepithelial $^{36}Cl^-$ fluxes from the apical to the basolateral bathing solution (J_{13}) and in the opposite direction (J_{31}). The potential dependence of fluxes obtained in Na^+-free choline Ringer's indicates the presence of conductive and nonconductive components that probably correspond to fluxes through paracellular and cellular pathways, respectively. Rectification of fluxes with reversal of the potential reflects a structural asymmetry, presumably in surface charge density. The data are consistent with a charge density of one negative charge per 280 Å^2 on the apical side. A new model for passive Cl^- transport was developed that includes surface charge asymmetry and specifically accounts for the observed variation of conductance with potential. In normal frog Ringer's, J_{13} was larger than J_{31} at zero potential (active Cl^- transport), J_{13} rose exponentially with increasing positive potential to reach a maximum at 40 mV (approximately open-circuit), and the predicted partial Cl^- conductance exceeded the measured conductance leading to the conclusion that when J_{13} is largely driven by Na^+ transport, much of the coupling occurs via nonconductive pathways. Theophylline stimulates Cl^- transport that also occurs via nonconductive pathways as V_t becomes more positive.

Introduction

Chloride transport across the frog skin has been ascribed to many different transport processes. Results obtained on skins of *Rana temporaria* and *Rana esculenta* led to the conclusion that Cl^- transfer across the frog skin occurs via simple electrodiffusion [1]. Measurements of Cl^- fluxes across the short-circuited skin of *Rana pipiens* at different Cl^- concentrations indicated that a large portion of the Cl^- flux is involved in an exchange diffusion or anion exchange process [2]. Most recently, evidence for exchange diffusion was also obtained in *R. esculenta* and *R. temporaria*, but only under conditions in which the transepithelial potential had a polarity which is opposite to the one occurring normally [3]. Large scale active transport of Cl^- in the inward direction was discovered in short-circuited skins of *Leptodactylus ocellatus* [4]. It has been known for some time that a very limited active transport in the inward direction can be observed in the *Rana* genus when the Cl^- concentration in the bathing solution is very low [5,6]. More recently an inward active transport has also been reported at the higher Cl^- concentrations contained in normal frog Ringer's solution [7–9].

The present study was undertaken to examine the role played by various transport systems in the overall transport of Cl^- across the frog skin. A study of the potential dependence of unidirectional fluxes was expected to provide information

Correspondence address: Dr. T.U.L. Biber, Medical College of Virginia, Box 551, MCV Station, Richmond, VA 23298, U.S.A.

about the presence and magnitude of diffusional and nondiffusional components of Cl^- fluxes. The effect of Na^+ and of theophylline on these transport processes was tested by carrying out experiments of Na^+-free choline Ringer's and in Ringer's with and without theophylline. In order to be able to make a quantitative comparison between the response of the influx with that of the efflux, the two fluxes were measured simultaneously on paired skins which had been obtained from the same frog and which were within 10% with respect to (i) the short-circuit current, (ii) the transepithelial resistance and (iii) the transepithelial potential.

The study indicates that the fluxes measured in Na^+-free Ringer's are made up of two components, one which involves simple diffusion and one which is potential-insensitive. Rectification of Cl^- fluxes measured at potentials different from zero and the potential dependence of conductance suggest a surface charge asymmetry. Addition of Na^+ (with or without theophylline) induces major nonconductive Cl^- pathways which become particularly dominant at the level of open-circuit potentials.

Methods

Frogs (*R. pipiens* of the Southern Variety) were killed by double pithing. Circular pieces of the abdominal skin were dissected and mounted in chambers which had been specifically designed to prevent edge-damage [10]. The techniques for voltage clamping and for measuring isotope fluxes have been described previously [11,12]. Briefly, the exposed area of isolated frog skin was 0.85 cm^2. The chambers on each side of the epithelium contained 0.5 ml bathing solution. The bathing solutions were connected to an automatic voltage clamp via agar bridges and calomel half-cells. The current was passed via Ag/AgCl electrodes and agar bridges. The automatic clamping device permits the voltage clamping of the epithelium at predetermined levels of transepithelial potential (V_t) and the application of square pulses which generates voltage steps of desired amplitude (usually $\pm$ 10 mV) and length (as short as 25 ms). The slope resistance (R_t) and the conductance (G) were calculated from the resulting changes in current. Readings of R (and G) were made at the end of 3 s pulses.

Transepithelial Cl^- fluxes were determined in the following way: $^{36}Cl^-$ was added to the bath on one side of the skin ('hot' side) and the accumulation of the tracer in the bath located on the other side of the epithelium ('cold' side) was used for the flux measurement once the appearance of the tracer had reached a steady state. At the end of each flux period, in a procedure which lasted less than 5 s, the chamber on the 'cold' side was emptied completely for collection $^{36}Cl^-$ and was refilled with fresh isotope-free solution. The duration of the individual sample periods was 15 min. Liquid scintillation spectrophotometry was used for counting $^{36}Cl^-$. Ion-selective electrodes were used for determination of Na^+, K^+, H^+ and Cl^- activities.

For the determination of bidirectional fluxes, the transepithelial Cl^- flux from apical to basolateral bath (Cl^- influx or J_{13}) and the flux in opposite direction (Cl^- efflux or J_{31}) were measured at the same time in carefully matched pairs of skins. Such pairs of skin were obtained from symmetrical locations in one frog and were accepted for bidirectional flux measurements only when all three parameters, the short-circuit current (I_o), R_t and open-circuit V_t, were within 10% for the two skins at the end of the equilibrium period.

The transepithelial potential difference, V_t, is defined as the potential in the basolateral bath minus the potential in the apical (i.e., outside) bath. V_t was voltage-clamped either at zero potential (control condition and during equilibration period) or at different potentials ranging from -60 to 60 mV except for the short times required to measure spontaneous V_t and R and to collect the fluid from the 'cold' side.

The following three conditions were used in this study: (i) Frog Ringer's solution (110 mM NaCl/2.5 mM $KHCO_3$/1 mM $CaCl_2$) bathing both sides of the epithelium; (ii) Same as (i) but 2.4 mM theophylline added to both sides; and (iii) Choline Ringer's solution (all Na^+ in frog Ringer's replaced by choline) bathing both sides of the skin.

Average values are given $\pm$ S.E. and numbers of observations are indicated in parentheses.

Model for fluxes and conductances in choline Ringer's

When the chloride influx and efflux are obtained under short-circuit conditions in the absence of Na^+, the data indicate that chloride ions are not actively transported. However, measurements at transepithelial potentials other than zero show that the fluxes are not due to simple electrodiffusion across an uniform symmetrical barrier. In the first place a marked rectification of the form:

$$J_{13}(V_t) \neq J_{31}(-V_t), \qquad V_t \neq 0 \tag{1}$$

is observed. Furthermore, the conductance varies with the applied potential. This would not be expected if the permeability barrier were structurally symmetrical and bathed by the same solution on both sides of the skin. Because choline has a low permeability (Drewnowska and Biber, unpublished observation), the entire conductance is dominated by chloride. Both the properties of rectification and the potential dependence of the conductance suggest that the passive electrodiffusion barrier is asymmetrical. In the case of electrolytes, the simplest form of asymmetry which can account for these properties is the surface charge density across the passive shunt barrier. However, in addition there is evidence for a nonconductive transcellular contribution to each unidirectional flux.

To find an appropriate explanation for the observed conductance changes and rectification of fluxes, a model is developed in which it is assumed that electrodiffusion across the shunt-barrier is biased by the presence of fixed negative surface charges at the apical entrance to the shunt. As described in more detail below, the model allows us to express the Cl^- influx as a linear function of a variable, r, which depends on both the surface potential and the transepithelial potential. The slope of the line is the conductive part of the Cl^- influx under short-circuit conditions, while the intercept (the flux at $r = 0$, or a V_t of minus infinity) represents the nonconductive part of the flux. A similar relation holds for the Cl^- efflux with r weighted by $\exp(-V_t/RT)$, where R is the gas constant and T is the absolute temperature.

Our goal is to derive expression for the fluxes and the conductance as a function of V_t with reasonable bounds on the surface potential and so separate both influx and efflux into conductive and nonconductive parts.

Flux equations

The simplest charge distribution with the necessary properties of asymmetry is an uniform negative surface charge associated with the apical side of the shunt. The permeability barrier within the shunt itself is assumed to be without fixed charge as is the basolateral-facing side. Fig. 1 shows a typical potential profile across the shunt. We have taken the potential to be zero in the apical bath, V_0 at the apical-facing entrance to the shunt barrier and V_t in the basolateral bath. V_0 is determined by the intrinsic properties of the fixed ionogenic anions. These are probably acidic moieties such as carboxyl groups, so that the negative fixed charge density is largely determined by the pH in the microenvironment. If we assume the charged and uncharged moieties are in equilibrium through a stoichiometric process involving proton binding, then the surface charge density, σ, is given by:

$$\sigma = -e\Gamma\left[1 + \frac{[H]}{K}e^{-\phi_0}\right]^{-1} \tag{2}$$

where e is the protonic charge, Γ is the density of ionogenic moieties per unit area, [H] is the hydro-

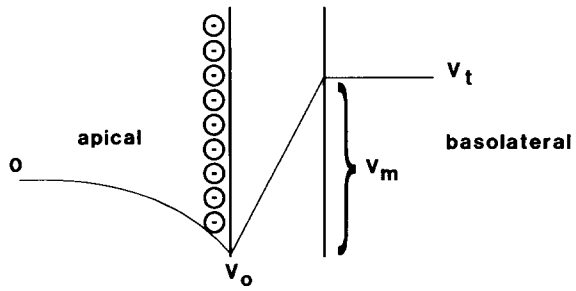

Fig. 1. A schematic of the potential across the shunt barrier presumed to be paracellular. The apical-facing side is assumed to have an uniform distribution of negative surface charge. V_0 is the apical surface potential determined by apical bath pH and salt concentration. V_t is the basolateral potential measured relative to an apical bath reference and is therefore the transepithelial potential. $V_t - V_0$ is the actual potential difference across the permeability barrier (V_m).

gen ion concentration in the apical bath, K is the dissociation constant of the proton dissociation reaction, and ϕ_0 is the normalized surface potential, $eV_0/\boldsymbol{k}T$, where e, $\boldsymbol{k}$ and T have their usual meanings.

The aqueous double layer region offers negligible resistance to ion movement relative to the shunt interior, so we can assume the apical interfacial region is in equilibrium with the apical bath. Assuming the apical bath to made up of 1 : 1 salts, Gouy-Chapman theory provides us with a second relation between the surface charge density and the surface potential, viz.:

$$\sigma = \sqrt{\frac{\varepsilon N c \boldsymbol{k} T}{500\pi}} \sinh \frac{\phi_0}{2} \tag{3}$$

where N is Avogadro's number, c the molar salt concentration in the apical bath, and ε, the dielectric constant of the medium. Eqns. 2 and 3 together determine ϕ_0 as an unique function of [H] and c. Because both [H] and c can be regarded as fixed, the surface potential can be considered constant.

Within the shunt we assume the laws of electrodiffusion apply. Making the usual constant field assumption, we arrive at the net chloride flux, J, viz.:

$$J = -Pz\phi_m c\, e^{-z\phi_0} \frac{(1 - e^{z\phi_t})}{(1 - e^{z\phi_m})} \tag{4}$$

where P is the permeability coefficient, c the chloride concentration on each side of the skin, $z = -1$, and:

$$\phi_m = eV_m/\boldsymbol{k}T$$

where $V_m = V_t - V_0$
and $\phi_t = eV_t/\boldsymbol{k}T$.
The unidirectional fluxes are therefore:

$$J_{13} = \frac{Pz\phi_m c\, e^{-z\phi_0}}{e^{z\phi_m} - 1} \tag{5a}$$

and

$$J_{31} = \frac{Pz\phi_m c\, e^{-z\phi_0}}{e^{z\phi_m} - 1} e^{z\phi_t} \tag{5b}$$

It is convenient to express J_{13} and J_{31} in terms of J^0, the value of J_{13} or J_{31} when $\phi_t = 0$ and $z = -1$, as is the case for chloride. Accordingly, it is readily shown that:

$$J_{13}(0) = J_{31}(0) = J^0 = \frac{P\phi_0\, e^{\phi_0} c}{e^{\phi_0} - 1} \tag{6}$$

so

$$J_{13} = J^0 r \tag{7a}$$

and

$$J_{31} = J^0 r\, e^{-\phi_t} \tag{7b}$$

where

$$r(\phi_t, \phi_0) = \frac{(\phi_0 - \phi_t)(e^{\phi_0} - 1)}{\phi_0 (e^{\phi_0 - \phi_t} - 1)} \tag{8}$$

If, the chloride flux includes a transcellular nonconductive part, $J'_{,}$ the flux equations become:

$$J_{13} = J^0 r + J' \tag{9a}$$

$$J_{31} = J^0 r\, e^{-\phi_t} + J' \tag{9b}$$

Here it has been assumed that both influx and efflux have nonconductive parts. However, this need not be the case, i.e., only one or the other flux may have a nonconductive part. In that case the transcellular flux of another ion must be invoked to insure that the additive component remains nonconductive.

The conductance

If the entire current is due to chloride,

$$I = zFJ \tag{10}$$

where I is the current, F, Faraday's constant, and J is the net chloride flux given by Eqn. 4. Under these conditions the chloride conductance and the measured slope conductance are the same. If we define the conductance, G, as:

$$G = -\frac{\partial I}{\partial V_t} \tag{11}$$

then

$$G = -\frac{I}{V_m}(1 - Q\, e^{-\phi_t}) + \frac{z^2 F^2}{RT} J_{31} \tag{12}$$

where

$$Q = \frac{z\phi_m e^{-z\phi_0}}{e^{z\phi_m} - 1} \tag{13}$$

Dividing Eqn. 12 by z^2F^2/RT produces a reduced conductance $\bar{G}$, with units of μequiv $\cdot$ h$^{-1}\cdot$ cm^{-2}, viz.,

$$\bar{G} = -\frac{RTI}{z^2F^2V_m}(1 - Qre^{-\phi_t}) + J_{31} \tag{14}$$

This is the form of the conductance which is used herein. It is also useful to define a dimensionless conductance, g, where

$$g = \bar{G}/Pc \tag{15}$$

This can be conveniently expressed as a function of ϕ_t and ϕ_0, viz.

$$g(\phi_t, \phi_0) = \frac{Q(e^{z\phi_t} - 1)}{z(\phi_t - \phi_0)}(1 - Q\,e^{z\phi_t}) + Q\,e^{z\phi_t} \tag{16}$$

If $\phi_0 = 0$, $g(\phi_t) = 1$, for all values of ϕ_t, i.e., the conductance of a symmetrical uncharged barrier is independent of the applied potential. This is not the case for the asymmetrical barrier considered here. Fig. 2 shows that the conductance decreases monotonically as the transepithelial potential passes from negative to positive values, provided $V_0 < 0$. This relation is in agreement with the data which show that the conductance varies in the predicted manner. Therefore the experimental behavior of the conductance serves as an independent confirmation of our initial assumption of a charge asymmetry.

Results

Experiments done in choline Ringer's

Chloride influx and efflux was measured in five paired skins at a V_t of -60, 0 and 60 mV. The results are listed in Table I. The influx and efflux determinations made under short-circuit conditions (i.e., $V_t = 0$) were not significantly different and therefore provide no information on active Cl^- transport. The flux asymmetry defined in Eqn. 1 is, however, evident.

The flux measurements were compared with the predictions made by Eqns. 9a and 9b for a variety of values of V_0 and α where α is defined as the ratio of the nonconductive part to the conductive part of the flux under short-circuit conditions. Among a number of combinations with different values for V_0 and α, two pairs of parameters provided good fits to both the flux data and the conductance data. These were: (i) $V_0 = -80$ mV, $\alpha = 0.2$ for both J_{13} and J_{31}, and (ii) $V_0 = -59$ mV for J_{13} and J_{31} with $\alpha = 0.4$ for J_{13} only. These parameters were used to construct the curves

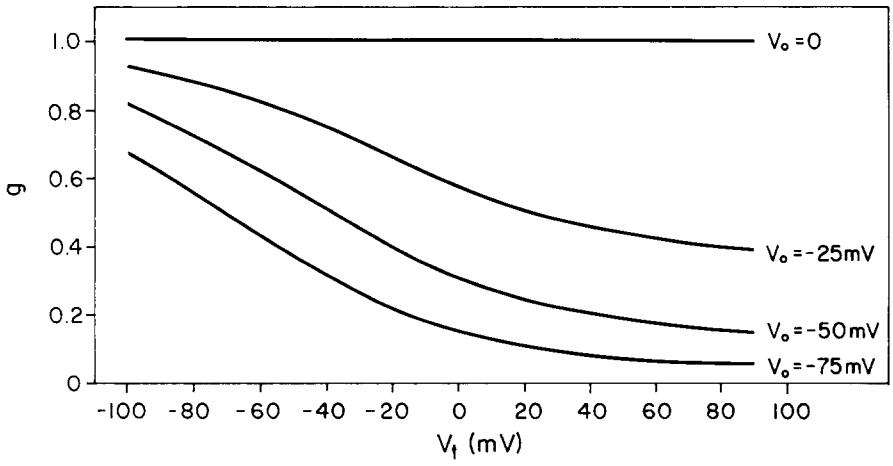

Fig. 2. A plot of the dimension conductance, g, against the transepithelial potential V_t for different values of the parameter V_0, the surface potential. Without surface charge, g is independent of potential. As V_0 increases g decreases monotonically in accord with the measured conductance.

TABLE I

FLUXES AND CONDUCTANCES OBTAINED IN CHOLINE RINGER'S SOLUTION: COMPARISON BETWEEN CALCULATED AND OBSERVED DATA

All values are in μequiv·h^{-1}·cm^{-2}, except for V_t, which is in mV. Data are either measured in experiments (labelled with m) or calculated (labelled with c). Calculations are based on $V_0 = -59$ mV and $\alpha = 0.4$ where $\alpha = J'/J^0$. The number of observations made at -60, 0 and 60 mV were 24, 24 and 18, respectively, for conductances ($\bar{G}_m$) and 12, 12 and 9, respectively, for each, Cl^- influx ($J_{13}{}^m$) and Cl^- efflux ($J_{31}{}^m$). For details see text.

V_t	$J_{13}{}^m$	$J_{13}{}^c$	$J_{31}{}^m$	$J_{31}{}^c$	$\bar{G}_m$	$\bar{G}_c$
−60	0.398 ± 0.022	0.396	2.886 ± 0.285	2.628	1.06 ± 0.05	1.40
−40		0.483		1.733		1.10
−20		0.588		1.088		0.82
0	0.710 ± 0.026	0.710	0.652 ± 0.077	0.652	0.60 ± 0.08	0.61
20		0.844		0.375		0.45
40		0.986		0.209		0.34
60	1.020 ± 0.063	1.134	0.109 ± 0.019	0.113	0.44 ± 0.07	0.28

shown on Figs. 3 and 4, respectively. In the case of Fig. 3 the fluxes are described by:

$$J_{13} = 0.592r + 0.118 \quad (17a)$$

$$J_{31} = 0.543r\, e^{-\phi_t} + 0.109 \quad (17b)$$

where the slopes represent the conductive part of the flux under short-circuit conditions and the intercepts define the nonconductive part of the flux. The differences between the fluxes obtained with this set of parameters and the observed fluxes are not significant. In the case of Fig. 4 the fluxes are given by:

$$J_{13} = 0.507r + 0.203 \quad (18a)$$

$$J_{31} = 0.652r\, e^{-\phi_t} \quad (18b)$$

The differences between the fluxes obtained with this second set of parameters and the observed fluxes are again not significant.

As shown in Table I, the conductance changed significantly with the value of V_t. In a symmetrical transport system the conductance would have been constant. The second set of parameters was used to calculate fluxes and conductances. These values are listed and compared with the observed data in Table I. It can be seen that the calculated fluxes agree well with all the corresponding experimental data and that the calculated conductance at zero potential concurs with the measured value. At −60 mV the calculated conductance exceeds the

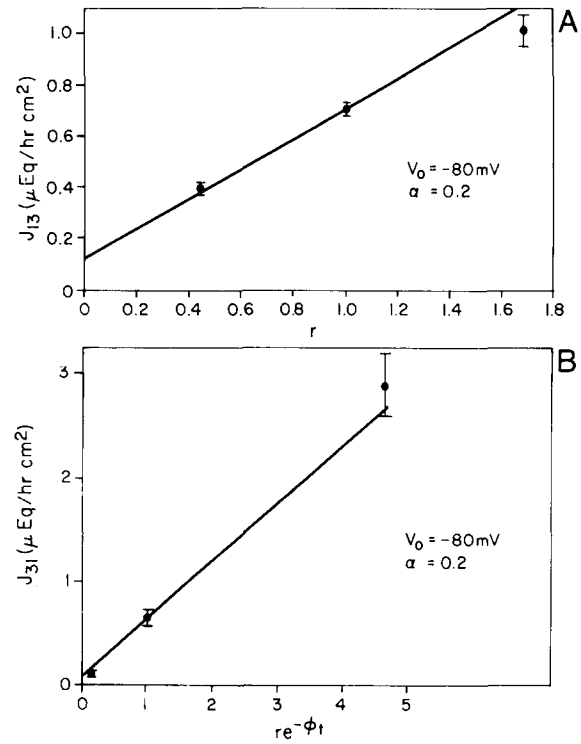

Fig. 3. (A) The Cl^- influx, J_{13}, plotted against a function r (ϕ_0, ϕ_t) derived in the text and defined by Eqn. 8. The slope is the conductive part of the flux, J_0, at $V_t = 0$ mV, which in this case equals 0.592. The intercept, J'/J_0 is 0.2. (B) The corresponding Cl^- efflux, J_{31}, as a function of $re^{-\phi_t}$. The surface potential is assumed to be −80 mV. Both J_{13} and J_{31} are assumed to have equal nonconductive parts.

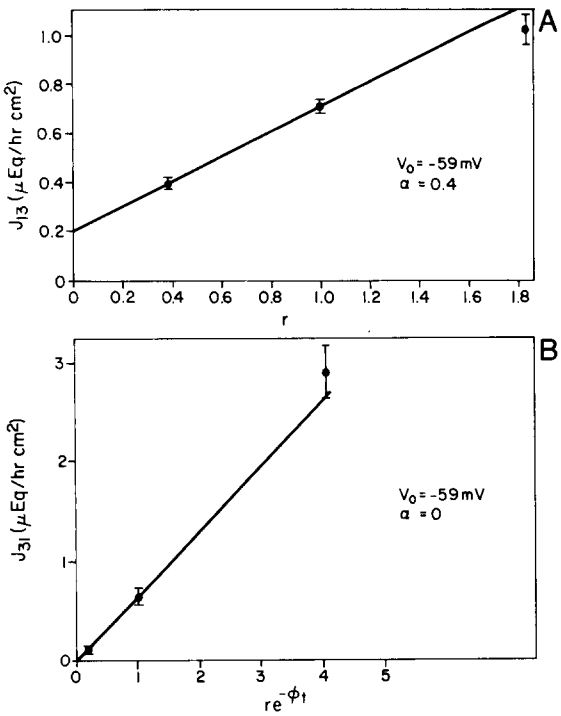

Fig. 4. The same as Fig. 3 except that $V_0 = -59$ mV and $\alpha = 0.4$. Note that in this case only J_{13} is assumed to have a nonconductive part.

corresponding observed value by 32% and at 60 mV the calculated conductance underestimates the measured value by 36%. However, the overall tendency of a decrease in conductance with increasingly positive transepithelial potentials is common to both the calculated and observed conductances and in view of the simplicity of the theory the agreement between calculated and measured data is quite remarkable.

As this approach provides us with a value for the surface potential it is possible to obtain an estimate for the surface charge density. Using Eqn. 3 and the values of -59 mV for the potential, 112 mM for Cl^- concentration and 79.6 for the dielectric constant, a surface charge density of one negatively charged moiety per 280 Å^2 is obtained.

Experiments done in frog Ringer's

In each of the 11 experiments reported here, Cl^- influx and efflux were determined on paired skins at 3–5 different levels of V_t. In the experiments in which the fluxes were measured at only three values of V_t, the flux determinations were made either at -40, 0 and 40 mV or at -60, 0 and 60 mV.

At V_t of 0, 40 and 60 mV the Cl^- influx was greater than the Cl^- efflux. The difference measured between the influx and efflux at zero V_t demonstrates active inward Cl^- transport (significant at $P < 0.01$). The average values of $\bar{G}$ (in μequiv. $\cdot$ h^{-1} $\cdot$ cm^{-2}) measured at -60, -40, 0, 40 and 60 mV were 0.72 ± 0.12 (46), 0.60 ± 0.14 (22), 0.79 ± 0.14 (50), 1.11 ± 0.20 (32), and 0.59 ± 0.08 (36), respectively.

The fluxes are plotted as a function of V_t in Fig. 5. The Cl^- influx is characterized by a sharp exponential rise as the potential changes from -60 mV to 40 mV. This is followed by a sharp

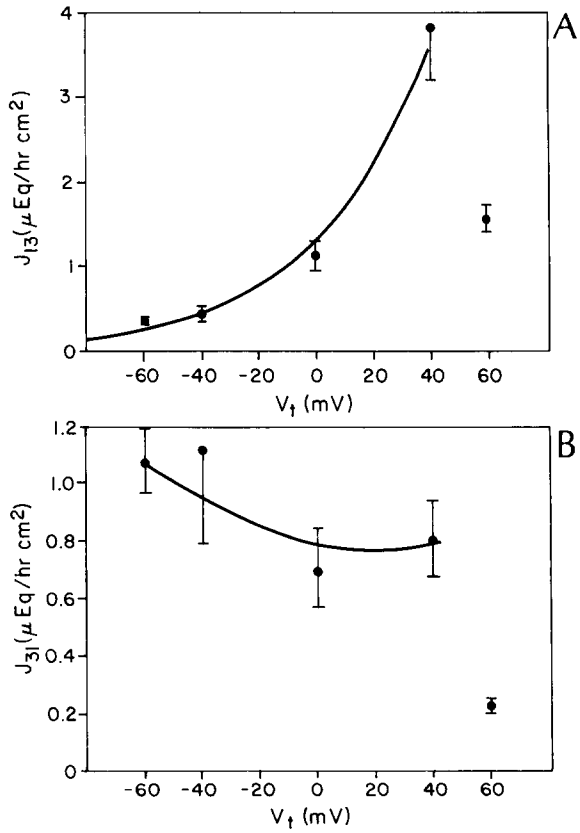

Fig. 5. (A) The Cl^- influx in frog Ringer's as a function of V_t. The curve was drawn according to Eqn. 19a. (B) The Cl^- efflux as a function of V_t. The curve was drawn according to Eqn. 19b.

drop as the potential is increased to 60 mV. The efflux, on the other hand, exhibits a trend to decrease slightly in the range from −60 mV and 40 mV and than also sharply declines at 60 mV. The smooth curves drawn between −60 mV and 40 mV for both influx and efflux were constructed using the following curve fitting procedure. It was assumed that passive conductive Cl^- fluxes found in choline Ringer's are probably paracellular (see Discussion) and as such are present also in normal frog Ringer's. The influx and efflux could then be considered to be composed of Na^+-dependent and Na^+-independent parts. The latter were assumed to be accurately represented by Eqns. 18a and 18b discussed in the previous section. The Na^+-dependent components were defined operationally as the difference between the measured fluxes at a given potential and the values calculated using Eqns. 18a and 18b. The Na^+-dependent component to both the Cl^- influx and efflux could in each case be represented by a single exponential function of V_t. The resulting expression for the fluxes are:

$$J_{13} = 0.734\, e^{0.89\phi_t} + 0.507 r(\phi_0, \phi_t) \tag{19a}$$

$$J_{31} = 1 - 0.86\, e^{-0.46\phi_t} + 0.652 r(\phi_0, \phi_t)\, e^{-\phi_t} \tag{19b}$$

As can be seen in Fig. 5, these equations apparently describe the data satisfactorily within the V_t range between −60 mV and 40 mV. To analyze and compare the potential dependence of the conductance for both the cases of choline Ringer's and frog Ringer's, the measured conductances are plotted in Fig. 6A. The open circles represent the conductance under choline Ringer's, already discussed in the previous section. The closed circles represent the conductance measured in frog Ringer's. It is seen that they vary respectively with potential in essentially opposite ways. Whereas as in the absence of sodium, $\bar{G}$ is a monotonically decreasing function of V_t between −60 mV and 60 mV, in the presence of sodium, $\bar{G}$ remains nearly constant between −60 mV and −40 mV, but then increases monotonically up to 40 mV before declining at 60 mV. If the sodium and chloride currents were independent at all potentials, the total conductance, $\bar{G}$, could then be represented as the sum of each partial conductance, viz.

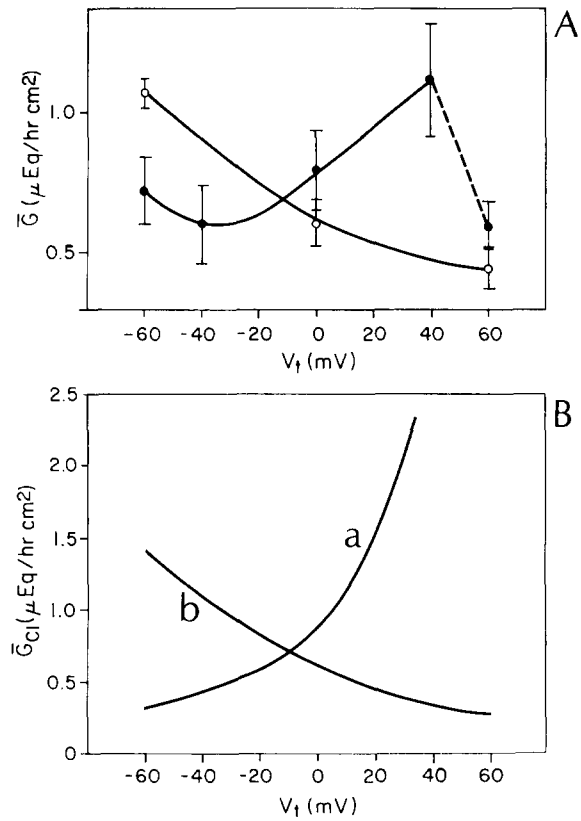

Fig. 6. (A) The measured slope conductance in choline Ringer's (open circles) and the measured slope conductance in frog Ringer's (closed circles). (B) Curve a is the calculated chloride partial conductance for the case of frog Ringer's derived from Eqns. 19a, 19b and 21, and curve b is the calculated chloride partial conductance for the case of choline Ringer's.

$$\bar{G} = \bar{G}_{Na} + \bar{G}_{Cl} \tag{20}$$

where $\bar{G}_{Na}$ is the sodium partial conductance and $\bar{G}_{Cl}$ is the chloride partial conductance. For simplicity, we ignore the small contributions of other ions. Of necessity, both $\bar{G}_{Na}$ and $\bar{G}_{Cl}$ are positive-definite.

Assuming independent ion pathways, the chloride partial conductance can be calculated from Eqns. 19a and 19b, viz.:

$$\bar{G}_{Cl} = \frac{\partial (J_{13} - J_{31})}{\partial \phi_t} \tag{21}$$

The results are plotted in Fig. 6B. Curve a shows

$\bar{G}_{Cl}$ in the presence of sodium. Comparing the experimentally determined $\bar{G}$ (closed circles Fig. 6A) and $\bar{G}_{Cl}$ we see that between -40 mV and 40 mV both are increasing functions of V_t. This is in sharp contrast to $\bar{G}$ and $\bar{G}_{Cl}$ in the absence of sodium, which we can readily see by comparing the measured $\bar{G}$ (open circles Fig. 6A) and the theoretically drawn curve b in Fig. 6B. However, whereas both $\bar{G}$ and $\bar{G}_{Cl}$ are in good quantitative agreement over the entire potential range in the absence of sodium, in its presence, Eqn. 20 does not describe the system. This is particularly clear as the potential approaches 40 mV, a value approximating the open-circuit potential. This is seen graphically by plotting the difference between the measured values of $\bar{G}$ and the calculated values of $\bar{G}_{Cl}$ here denoted $\bar{G}_e$. $\bar{G}_e$ would be positive-definite and equal to $\bar{G}_{Na}$ were the sodium and chloride fluxes strictly conductive and independent. Fig. 7 shows that, whereas at -60 mV and -40 mV $\bar{G}_e$ is positive, the minimum necessary requirement for the validity of Eqn. 20, at 0 mV and 40 mV, $\bar{G}$ is negative. The chloride partial conductance exceeds the total conductance implying an impossible negative value of $\bar{G}_{Na}$. This indicates that as the system approaches open-circuit increasingly more of the chloride flux cannot be attributed to simple electrodiffusion. Of course, at open-circuit the sodium and chloride fluxes must be equal. It appears that the steep increase in J_{13} as V_t approaches 40 mV is related to such obligatory coupling. Thus, at open-circuit and to a lesser extent at short-circuit, chloride must follow pathways which result in an overall lowering of the conductance relative to that expected for simple electrodiffusion. Under open-circuit conditions, when the potential is a result of active transcellular sodium transport, chloride is constrained to follow pathways which are less conductive or perhaps altogether nonconductive. These are most probably also transcellular routes. While the observed conductance and the predicted chloride partial conductance do increase in parallel fashion over the interval -40 mV $< V_t <$ 40 mV, the latter exceeds the former by 153%. This is evidence of specific coupling between sodium and chloride fluxes and good indication that the coupling includes nonconductive elements.

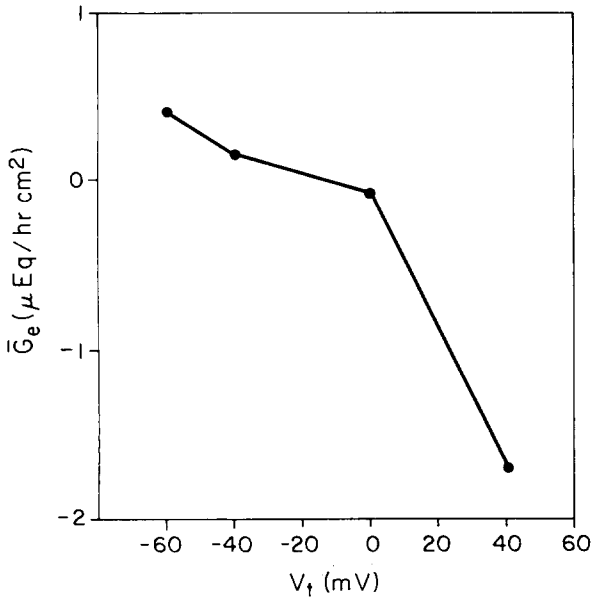

Fig. 7. The difference between the measured conductance and the chloride partial conductance, $\bar{G}_e$, as a function of V_t. Note that $\bar{G}_e$ is negative for all positive values of V_t, a condition which violates the assumption of independence of sodium and chloride fluxes.

Experiments done with theophylline added to frog Ringer's

A third series of experiments was carried out under conditions in which 2.4 mM theophylline in frog Ringer's had been added to both sides of the epithelium. As in the other experiments, the Cl^- influx and efflux were measured simultaneously on paired skins. In three of the four experiments done in this series, flux measurements were made at five levels of V_t. In one experiment, fluxes were determined only at -60 mV. The fluxes obtained at each value of V_t are given in Table II. The values of $\bar{G}$ (in μequiv $\cdot$ h^{-1} $\cdot$ cm^{-2}) measured at the potentials (in mV) of -60, -40, 0, 40 and 60 were: 1.31 ± 0.17, 1.60 ± 0.25, 2.09 ± 0.94, 2.19 ± 0.25, and 2.48 ± 0.33, respectively.

Except for the Cl^- efflux at -40 mV, the fluxes are significantly higher than those observed in frog Ringer's alone. Comparison of the fluxes in Table II and the conductance above with those obtained in frog Ringer's indicates the same quantitative behavior. It is clear that here, too, the predicted chloride partial conductance will exceed the measured conductance as the potential be-

TABLE II

CHLORIDE FLUXES MEASURED AT DIFFERENT V_t IN FROG RINGER'S SOLUTION TO WHICH 2.4 mM THEOPHYLLINE HAD BEEN ADDED

J_{13} and J_{31} obtained in four pairs of skins at different levels of transepithelial potential (V_t). Fluxes in $\mu equiv \cdot h^{-1} \cdot cm^{-2}$ and V_t in mV.

V_t	J_{13}	J_{31}
−60	1.069 ± 0.231 (12)	3.383 ± 0.304 (12)
−40	1.232 ± 0.257 (9)	2.988 ± 0.691 (7)
0	4.118 ± 0.777 (7)	2.723 ± 0.420 (9)
40	7.012 ± 0.978 (9)	1.833 ± 0.223 (9)
60	9.449 ± 1.377 (10)	1.381 ± 0.233 (10)

comes increasingly more positive. As before this implies the presence of nonconductive pathways for chloride. The significantly higher fluxes suggests that theophylline promotes additional nonconductive pathways.

Discussion

In sodium-free choline Ringer's solution no net movement of Cl^- can be observed when the transepithelial potential (V_t) is zero, i.e., when no external driving force is present. This is in agreement with the notion that, under these conditions, the transepithelial Cl^- movement is passive. The fact that the Cl^- fluxes display rectification with respect to reversal in V_t suggests, however, that at least one barrier along the transport pathway is asymmetrical. The failure to obey the flux ratio equation, observed previously [9] and in this study at −60 mV, is consistent with the idea and also indicates the possibility of nonconductive components to the flux along the lines of exchange diffusion. Further evidence suggesting an asymmetrical transport barrier arises from the dependence of the conductance on the potential.

As we have shown, it is possible to explain these data with a relatively simple model. In this model the asymmetry is attributed to a fixed negative surface charge associated with the apical surface of the tissue and the assumptions are made (i) that in absence of sodium the major Cl^- transport barrier is a conductive paracellular shunt and (ii) that the Cl^- influx and/or efflux may have a minor transcellular nonconductive component. The concept of assigning conductive and nonconductive elements of the Cl^- flux to paracellular and transcellular pathways, respectively, is supported by a recent study of Cl^- movement across cell membranes in which no evidence for Cl^- conductance was found in the apical or basolateral cell membrane [13]. This observation permits the conclusion that transcellular Cl^- transfer across granular cells proceeds via nonconductive pathways and that conductive Cl^- movement involves therefore only paracellular pathways or the much less abundant mitochondria-rich cells (see below). The model is basically an electrodiffusion model with the surface potential chosen to maximize agreement between the theoretically generated flux components and the observations. An additional constraint on the surface potential and nonconductive components (if present) is the requirement of predicting the conductance relation. Our best choice of parameters indicates that the Cl^- influx has a nonconductive part amount to about 40% of the total influx under conditions of zero transepithelial potential. The calculated density of negative charge in the vicinity of the apical barrier is one per 280 $Å^2$. It is not known whether this density extends out beyond the regions of the cell junctions and also includes the cellular transport sites. It should be noted, however, that the calculated surface charge density is of the same order as that estimated for the outer surface of squid giant axon. In the latter case a density of one negative charge for 120 $Å^2$ has been reported, with a lower limit of one charge per 280 $Å^2$ [14].

The model itself is similar to those introduced by DeSimone and Price [15], and more recently by Blank [16] and by Lindemann [17]. The form of Eqns. 9a and 9b is suggestive of the treatment of paracellular ion transport by Frizzell and Schultz [18] in that both theories arrive at transformations of the potential which results in linearizations of the unidirectional flux equations with the conductive part of the flux at short-circuit conditions as the slope and the nonconductive part as the intercept. However, the Frizzell-Schultz treatment is based upon the assumption of a potential independent conductance and therefore could not be used as such. In that sense, our treatment can be considered to be a generalization of theirs to in-

clude cases where the assumption of constant conductance must be relaxed.

The passive rectifying properties may be those of an asymmetrical paracellular shunt. By this we do not rule out the possibility that some or all chloride transport may take place across mitochondria-rich cells, as suggested by Voute and Meier for the frog skin [19] and by Larsen and co-workers in case of the toad skin [20–22]. The hypothesis of involvement of surface charges could play a dominant role even if chloride transport proceeded exclusively through the mitochondria-rich cells.

In experiments done on skins from *R. temporaria* and *R. esculenta*, Kristensen noted that many preparations have dramatic rectifying properties resulting in an large increase in G when the transepithelial potential is shifted from zero to a positive value of some 100 to 120 mV [3]. * This is in sharp contrast to the experiments on the Southern Variety of *R. pipiens* presented here, since we observe the opposite, namely that an overall change in V_t from 0 to +60 mV is accompanied by a decrease in conductance: In choline Ringer's, G at 60 mV is lower than at zero potential, the same is the case in frog Ringer's except that the decline in G is interrupted by a larger G at 40 mV. This tendency of a decline in G between these potential levels is in agreement with previous observations made by Helman and Fisher on *R. pipiens* of Southern origin [23]. Thus, there are major discrepancies between the observations of Kristensen on *R. temporaria* and *R. esculenta* [3] and those found by us on the Southern Variety of *R. pipiens*: In the former two species the Cl^- transport exhibits characteristics of exchange diffusion at negative transepithelial potentials but not at zero or at positive potentials, whereas in the latter exchange diffusion properties can be observed at zero and at positive potentials [2,9]. Furthermore, and perhaps most significant, is the fact that skins of the Southern Variety of *R. pipiens* exhibit in presence of Na^+ substantial active inward movement of Cl^- at high external Cl^- concentrations [7,9], a property that has not been observed in *R. temporaria* or *R. esculenta*. Furthermore, it should be noted that the experimental conditions used by Kristensen [3] are different from the ones employed in this study: Kristensen's measurements were made in frog Ringer's to which amiloride had been added. It is known, however, that amiloride causes changes in paracellular shunt conductance [24].

There are substantial changes in chloride fluxes where Na^+ is added to the bathing solution: the chloride influx increases at zero potential and at positive transepithelial potentials, and the chloride efflux decreases at −60 mV and increases at +60 mV. The effect of the presence of Na^+ in the bath on chloride fluxes is not unexpected, since previous studies on the short-circuited skin of *R. pipiens* have revealed a decrease in chloride flux when Na^+ is removed from the bath or when Na^+ transport is blocked with amiloride [9,25,26]. The observation that there is in presence of Na^+ net inward chloride transport under short-circuit conditions confirms previous observations in *R. pipiens* [7,8,9] and in *L. ocellatus* [27,28]. A remarkable aspect of Cl^- transport by tissue exposed to Na^+ is the appearance of a nearly exponential increase in the Cl^- influx as the potential is changed over a range from −60 mV to 40 mV. Indeed the influx is more than 10-times greater at 40 mV than at −60 mV. This is in marked contrast to the increase in Cl^- influx observed in choline Ringer's, which amounts to an about 2.5-fold increase between the same potentials. The apparent reason for this is the additional driving force supplied by the active influx of Na^+. In the absence of Na^+, any potential different from zero must be achieved by passing current from an external source. With Na^+ present, the zero current state corresponds, of course, to a large positive potential, the open-circuit potential. In these experiments this was of the order of 40 mV. Therefore the rapid rise in the Cl^- influx coincides with the passage of the system from short-circuit to open-circuit.

The influx and efflux data can be decomposed into sodium-dependent and sodium-independent parts. Within the transepithelial potential range between −60 mV and 40 mV the sodium-dependent parts of both the influx an the efflux are

* For the purpose of this discussion we refer here and in the following text to V_t as defined in the Methods section, although Kristensen [3] as well as Larsen and co-workers [20–22] used a definition of V_t which is opposite in sign.

described mathematically by single exponential functions of the potential. Therefore Eqns. 19a and 19b enable us to calculate the Cl^- partial conductance. As seen in Fig. 6, the calculated conductance overpredicts the measured conductance by more than 150%. This indicates that the Na^+ and Cl^- fluxes are coupled and that a substantial part of the Cl^- flux is nonconductive. The coupling must also be present under short-circuit conditions as indicated by the negative value of $\overline{G}_c$ in Fig. 7 at V_t equal to zero. It should be stressed that the Cl^- flux reaches a maximum at 40 mV, but, as the analysis shows, the nonconductive alternative pathways predominate under these conditions.

Our finding that in the presence of sodium the chloride influx increases nearly exponentially with potential between −60 mV and 40 mV is qualitatively similar to observations made on the toad skin [20,21]. The presence of sodium also results in an overall increase in conductance with potential. Larsen and Rasmussen [22] have modelled these conductance increases in terms of voltage-gated apical chloride channels located exclusively in the mitochondria-rich cells. However, the existence of voltage-gated chloride channels of the Hodgkin-Huxley type, which presumably obey the independence principle, is in our case doubtful because of the strong coupling to the flux of sodium. We have accordingly adopted an empirical approach to the modeling of the sodium-dependent behavior of the system. The exponential increase in chloride influx does produce a calculated chloride-conductance which varies qualitatively like the measured conductance. However, it quantitatively overestimates the conductance confirming that the sodium and chloride fluxes are not strictly independent in the Hodgkin-Huxley sense. It appears that the nature of the coupling involves nonconductive modes of chloride transfer. At 60 mV there is both a drop in Cl^- influx and a fall in conductance. The reason for this is not known, but it is conceivable that a decoupling of Na^+ and Cl^- fluxes occurs because the additional adverse potential impedes Na^+ influx across the apical barrier. This decoupling does not appear to occur in theophylline-treated skins. However, similar rapid increases in fluxes that proceed presumably via nonconductive pathways can be observed, particularly as increasing more positive potentials are imposed.

Acknowledgements

The authors would like to thank Mrs. K. Piette and Mrs. E. Dixon for valuable technical assistance. This work was made possible by support from NIH grant AM 26347.

References

1 Kristensen, P. (1978) J. Membrane Biol. 40S, 167–185
2 Biber, T.U.L., Walker, T.C. and Mullen, T.L. (1980) J. Membrane Biol. 56, 81–92
3 Kristensen, P. (1983) J. Membrane Biol. 72, 141–151
4 Zadunaisky, J.A. and Candia, O.A. (1962) Nature (London) 195, 1004
5 Martin, D.W. and Curran, P.F. (1966) J. Cell Physiol. 67, 367–374
6 Kristensen, P. (1972) Acta Physiol. Scand. 84, 338–346
7 Watlington, C.O. and Jessee, F. (1975) Biochim. Biophys. Acta 382, 204–212
8 Watlington, C.O., Jessee, F. and Baldwin, G. (1977) Am. J. Physiol. 232, F550–F558
9 Drewnowska, K. and Biber, T.U.L. (1985) Am. J. Physiol. 249, F424–F431
10 Biber, T.U.L. and Mullen, T.L. (1977) Am. J. Physiol. 232, C67–C75
11 Biber, T.U.L. and Saunders, M.L. (1973) J. Gen. Physiol. 61, 529–551
12 Biber, T.U.L. and Mullen, T.L. (1976) Am. J. Physiol. 231, 995–1001
13 Biber, T.U.L., Drewnowska, K., Baumgarten, C.M. and Fisher, R.S. (1985) Am. J. Physiol. 249, F432–F438
14 Gilbert, D.L. and Ehrenstein, G. (1969) Biophys. J. 9, 447–463
15 DeSimone, J.A. and Price, S. (1976) Biophys. J. 16, 869–881
16 Blank, M. (1983) Bioelectrochem. Bioenerg. 10, 451–465
17 Lindemann, B. (1982) Biophys. J. 39, 15–22
18 Frizzell, R.A. and Schultz, S.G. (1972) J. Gen. Physiol. 59, 318–346
19 Voute, C.L. and Meier, W. (1978) J. Membrane Biol. 40, 141–165
20 Willumsen, N.J. and Larsen, E.H. (1985) in Transport Processes, Iono- and Osmoregulation (Gilles, R. and Gilles-Baillien, M., eds.), pp. 20–30, Springer-Verlag, Berlin
21 Katz, U. and Larsen, E.H. (1984) J. Exp. Biol. 109, 353–371
22 Larsen, E.H. and Rasmussen, B.E. (1985) Pflügers Arch. 405, S50–S58
23 Helman, S.I. and Fisher, R.S. (1977) J. Gen. Physiol. 69, 571–604
24 Nagel, W., Garcia-Diaz, J.F. and Essig, A. (1983) Pflügers Arch. 399, 336–341
25 Macey, R.I. and Meyers, S. (1963) Am. J. Physiol. 204, 1095–1099
26 Candia, O.A. (1978) Am. J. Physiol. 234, F437–F445
27 Ques-von Petery, M.V., Rotuno, C.A. and Cereijido, M. (1978) J. Membrane Biol. 42, 317–330
28 Rotunno, C.A., Ques-von Petery, M.V. and Cereijido, M. (1978) J. Membrane Biol. 42, 331–343